

**REPORT DOCUMENTATION PAGE**Form Approved  
OMB NO. 0704-0188

Public Reporting burden for this collection of information is estimated to average 1 hour per response, including the time for reviewing instructions, searching existing data sources, gathering and maintaining the data needed, and completing and reviewing the collection of information. Send comment regarding this burden estimate or any other aspect of this collection of information, including suggestions for reducing this burden, to Washington Headquarters Services, Directorate for Information Operations and Reports, 1215 Jefferson Davis Highway, Suite 1204, Arlington, VA 22202-4302, and to the Office of Management and Budget, Paperwork Reduction Project (0704-0188,) Washington, DC 20503.

1. AGENCY USE ONLY (Leave Blank)

2. REPORT DATE  
June 20, 20003. REPORT TYPE AND DATES COVERED  
Final Technical Report4. TITLE AND SUBTITLE  
Dynamic Constitutive and Failure Characterization of Rate Sensitive Alloys5. FUNDING NUMBERS  
DAAH04-93-G-00376. AUTHOR(S)  
Dr. Ares J. Rosakis and Dr. G. Ravichandran7. PERFORMING ORGANIZATION NAME(S) AND ADDRESS(ES)  
The California Institute of Technology  
Office of Sponsored Research MS 213-6  
1200 E. California Blvd.  
Pasadena, CA 911258. PERFORMING ORGANIZATION  
REPORT NUMBER

9. SPONSORING / MONITORING AGENCY NAME(S) AND ADDRESS(ES)

U. S. Army Research Office  
P.O. Box 12211  
Research Triangle Park, NC 27709-221110. SPONSORING / MONITORING  
AGENCY REPORT NUMBER

ARO 28961.1-EG

## 11. SUPPLEMENTARY NOTES

The views, opinions and/or findings contained in this report are those of the author(s) and should not be construed as an official Department of the Army position, policy or decision, unless so designated by other documentation.

12 a. DISTRIBUTION / AVAILABILITY STATEMENT

Approved for public release; distribution unlimited.

12 b. DISTRIBUTION CODE

## 13. ABSTRACT (Maximum 200 words)

The objectives of this research program are (1) to establish critical conditions for initiation and growth of adiabatic shear bands in pre-notched plates subjected to asymmetric impact loading and (2) investigate the transition between competing failure modes under varying loading conditions. Typically, failure under asymmetric loading may occur by either dynamic cracking or adiabatic shear banding, both of which may be observed in the same specimen or structure depending on the instantaneous local stresses. In this stage of the research program, specimens of a high strength maraging steel, C300 were studied in two different geometries consisting of either a single pre-notch or two parallel notches. The investigation of different specimen geometries was motivated by discrepancies reported in the literature regarding failure mode selection in maraging steels.

20001122 081

14. SUBJECT TERMS  
Dynamic Failure, Shear Banding, High Strength Alloys

15. NUMBER OF PAGES

16. PRICE CODE

A Final Report on

**DYNAMIC CONSTITUTIVE AND FAILURE CHARACTERIZATION OF RATE  
SENSITIVE ALLOYS**

**Contract Number: DAAH04-93-G-0037**

**By**

**Ares J. Rosakis and G. Ravichandran**  
Graduate Aeronautical Laboratories  
California Institute of Technology  
Pasadena, California 91125

**Submitted to**

**Army Research Office**  
4300 South Miami Blvd.  
P.O. Box 12211  
Research Triangle Park, North Carolina 27709-2211

## 1. Objective and Approach

The objectives of this research program are (1) to establish critical conditions for initiation and growth of adiabatic shear bands in pre-notched plates subjected to asymmetric impact loading and (2) investigate the transition between competing failure modes under varying loading conditions. Typically, failure under asymmetric loading may occur by either dynamic cracking or adiabatic shear banding, both of which may be observed in the same specimen or structure depending on the instantaneous local stresses. In this stage of the research program, specimens of a high strength maraging steel, C300 were studied in two different geometries consisting of either a single pre-notch or two parallel notches as shown in Fig. 1. The investigation of different specimen geometries was motivated by discrepancies reported in the literature regarding failure mode selection in maraging steels. Kalthoff and co-workers [1,2] using the doubly notched specimens reported that failure occurred by either cracking at low impact velocities or shear banding at high velocities. Rosakis, Ravichandran and co-workers [3-5] on the other hand observed an intermediate impact velocity range where failure occurred initially by a shear band which arrested, followed by the formation of a dynamic crack. Experimental observations were made high speed infrared temperature measurements using a linear array of 16 detectors mapped perpendicular to the notch axis at a distance of 3 or 6 mm from the initial notch. Full-scale thermomechanical finite element simulations were conducted to compliment the experimental study and aid in the development of appropriate criteria for shear band initiation and propagation. Material parameters used in the simulations were measured in separate constitutive testing conducted over a broad range of conditions. The combined experimental – numerical approach allows for direct comparison between experimental observations and numerical predictions obtained using a variety of material constitutive models and failure criteria.

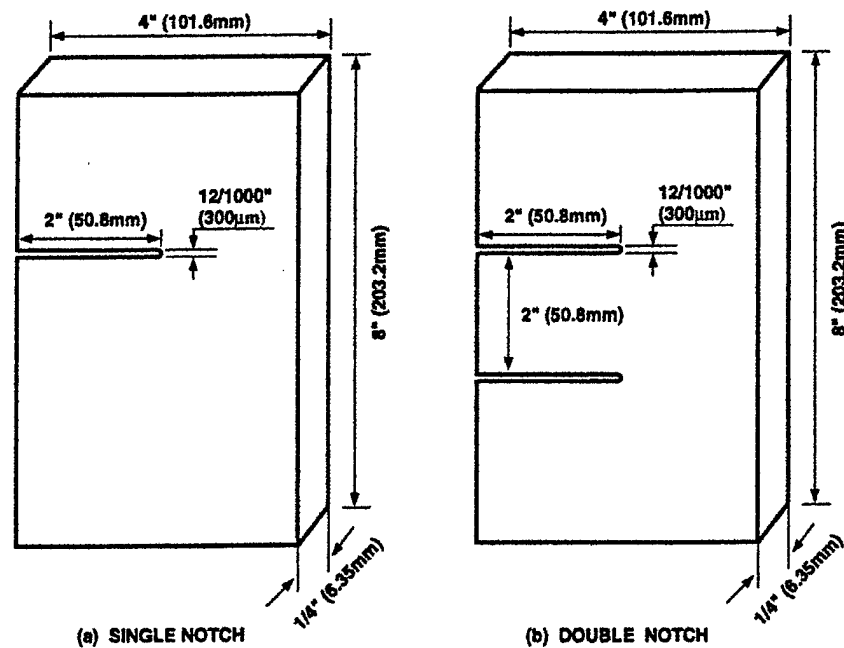


**Figure 1** Configurations used in the investigation of the role of specimen geometry on shear band initiation and propagation: (a) single notch and (b) double notch.

## 2. Accomplishments

The material used in the study of geometrical effects on shear band initiation and propagation was a Ni-Co-Mo maraging steel, C300. Sheet specimens of the material were cut and notched as shown in Fig. 1 and were then subsequently heat treated to the peak aged condition (755 K for 4 hours, then air-cooled). Experimental observations and numerical simulations showed that loading rate dramatically influences shear band initiation and the subsequent temperature distribution across the band and its propagation speed. It was also shown that shear band arrest and subsequent crack initiation and growth occurred in both singly and doubly notched specimens when the impact velocity was reduced to below a critical value.

### 2.1 Observed Failure Modes

Figures 2 and 3 summarize the failure modes observed in singly and doubly notched specimens, respectively. In both configurations, it is apparent that essentially identical failure behavior occurred. When the impact velocity was below a critical value, shear bands were observed to arrest. Following arrest, a crack initiated from the end of the shear band and propagated at an angle of  $30^\circ$  with respect to the path of the shear band.

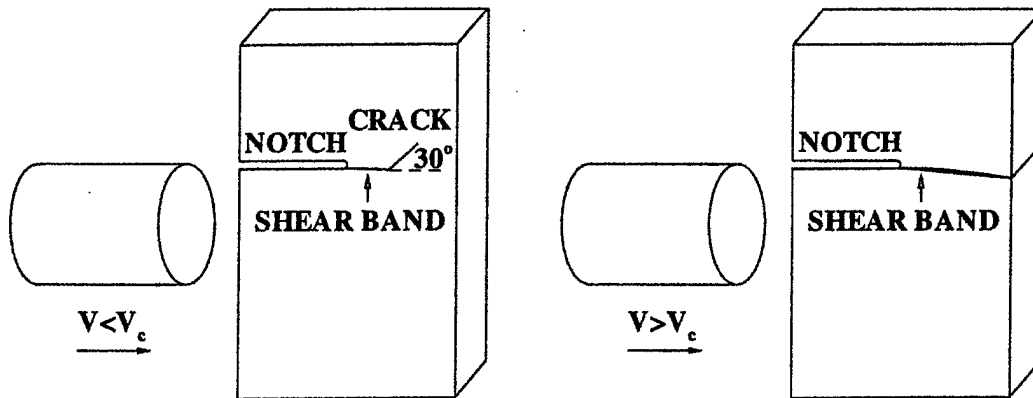


**Figure 2** Observed failure modes in singly notched C300 specimens. At impact velocities below a critical value, the shear band arrested within the specimen and a crack subsequently initiated at an angle of  $30^\circ$  with respect to the path of the shear band.

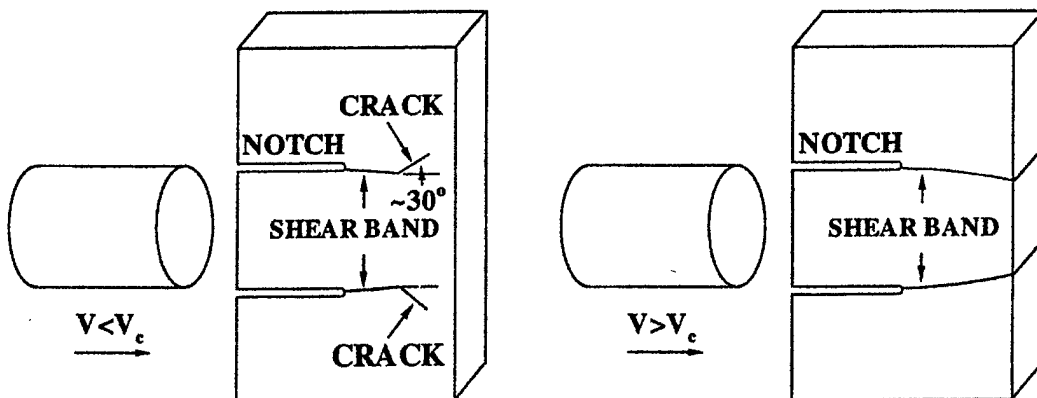


**Figure 3** Observed failure modes in doubly notched C300 specimens. In a manner identical to the singly notched specimens, at impact velocities below a critical value, the shear bands arrested within the specimen and a crack subsequently initiated at an angle of  $30^\circ$  with respect to the path of the shear band.

The observation of a crack or cracks initiating from the end of an arrested shear band does not agree with the observations of Kaltoff and co-workers [1,2] where failure occurred by either shear banding or cracking, but never both in the same specimen. It was observed that cracks propagated at an angle of  $70^\circ$  with respect to the notch axis, which is in agreement with predictions for the direction of propagation of cracks loaded in pure mode II. Although the compositions of the steels used in both studies are essentially identical, the mechanical properties (e.g. yield stress, hardening exponent, tensile strength) may vary significantly as a result of heat treatment which may result in the observed differences in failure modes.

## 2.2 Observed Temperature Profiles

The linear array of 16 InSb detectors,  $80\text{ }\mu\text{m}$  square and spaced  $100\text{ }\mu\text{m}$  apart were mapped onto the specimen surface on a line perpendicular to the initial notch axis at a distance of  $3\text{ mm}$  from the initial notch tip. The optical system used had a magnification of 1 and therefore, the temperatures reported for each detector represent an average temperature measured over an area of  $80\text{ }\mu\text{m}^2$ . The detectors are only sensitive to temperatures above approximately  $410\text{ K}$  for the C300 steel. Temperature profiles recorded at different distances from the initial notch were similar indicating that the shear band can be treated as a self-similar entity over the spatial and temporal scales relevant to this study. Figure 4 shows three temperature profiles to illustrate the influence of notch geometry and impact velocity. The profiles shown in Fig. 4a and 4b were recorded from specimens having a one and two notches, respectively and loaded with a projectile at a velocity  $27\text{ m s}^{-1}$ . Figure 4c illustrates a typical profile for a doubly notched specimen loaded by a projectile having a velocity of  $40\text{ m s}^{-1}$ .

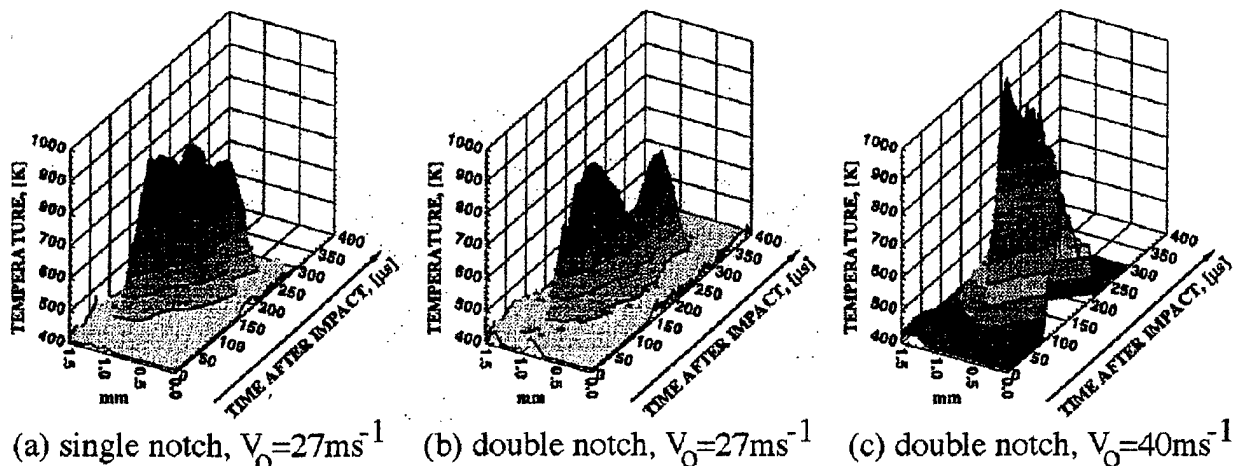


**Figure 4** Temperature profiles recorded using a linear array of 16 InSb infrared temperature detectors mapped perpendicular to the initial notch axis at a distance of  $3\text{ mm}$  from the initial notch tip.

Comparing Figs. 4a and 4b it is apparent that the peak temperatures of  $980\text{ K}$  and  $910\text{ K}$  are fairly similar for the singly and doubly notched specimens, respectively. Furthermore, the overall shape of the profiles are essentially identical at times up to  $200\text{ }\mu\text{s}$  after impact. At later times, the temperatures measured are significantly behind the tip of the propagating shear band, and as a result are not relevant to the investigation of shear band properties. Indeed Zhou, Ravichandran and Rosakis [5] showed that shear loading conditions favorable to shear band initiation and propagation diminish in this configuration at times exceeding  $200\text{ }\mu\text{s}$ . The influence of impact velocity on shear band temperatures is apparent from the comparison of Figs.

4b and 4c, where the peak temperature increases from 910 to 1210 K when the impact velocity is increased from 27 to 40 m s<sup>-1</sup>. Again this observation is consistent with the earlier observations on singly notched specimens of Zhou, Rosakis and Ravichandran [4], where a higher loading rate resulted in higher propagation velocities and temperatures. In summary, the experimental results obtained on the two specimen geometries reveal that choice of configuration does not lead to significant changes in shear band characteristics.

### 2.3 Numerical Analysis

The approach used for the analysis of the doubly notched specimen configuration follows that reported previously in the work of Zhou and co-workers [5,6]. The simulations consider fully coupled thermo-mechanical processes during dynamic deformation and utilizes the generalized  $J$ -integral for dynamic conditions presented by Moran and Shih [7,8]. Calculations of  $J$  for the two configurations remained identical up until the time when stress wave reflections from specimen edges or second notch (in the doubly notched specimen) began to interact with the notch tip under consideration. After the onset of such interaction, the  $J$  values in the doubly notched specimens were slightly lower, representing a lower driving force for crack or shear band initiation in comparison to the singly notched specimens. As a result, the time for initiation of a shear band is slightly longer in the doubly notched specimen (25  $\mu$ s versus 21  $\mu$ s). However, the level of  $J_c$  for initiation is the same in both cases and had a value of 115 kJ m<sup>-3</sup>, suggesting that the value of  $J$  at shear band initiation may be an appropriate measure of a material's resistance to shear band initiation. The interaction between the two notches in the doubly notched specimens (causing a diminished driving force) also led to a relative decrease in the simulated shear band velocity when compared to a singly notched specimen loaded under identical conditions. This difference in velocity would account for the similar, but slightly lower, peak temperature measured in the doubly notched specimens as illustrated in Figs. 4a and 4b.

Figure 5 shows a comparison of the numerical results obtained from both the singly and doubly notched specimens at two different time steps (30 and 40  $\mu$ s after impact), plotting the in-plane shear stress component in the region near the initial notch tip (loading occurs below the notch in the simulations). Overall, the stress fields are similar in the two configurations with slightly lower stresses occurring in the doubly notched specimens at the later times which was also evidenced by the lower values of  $J$ . Temperature fields were also evaluated from the simulations and the peak temperatures from the simulations agreed with the experimentally observed profiles (see Fig. 4) to within 25 K. The observation of slightly lower temperatures in the doubly notched specimen was replicated in the numerical results.

### 3. Summary

An investigation of the role of specimen geometry on shear band initiation and growth indicated that the use of singly or doubly notched specimens has essentially no influence on the observed failure modes or temperature profiles. Therefore, specimen geometry cannot be used to reconcile discrepancies reported in the literature regarding shear band characteristics in C300 maraging steel. Instead, it is concluded that differences in material properties resulting from different heat treatments of steels having nominally identical composition is the primary reason for changes in shear band characteristics.

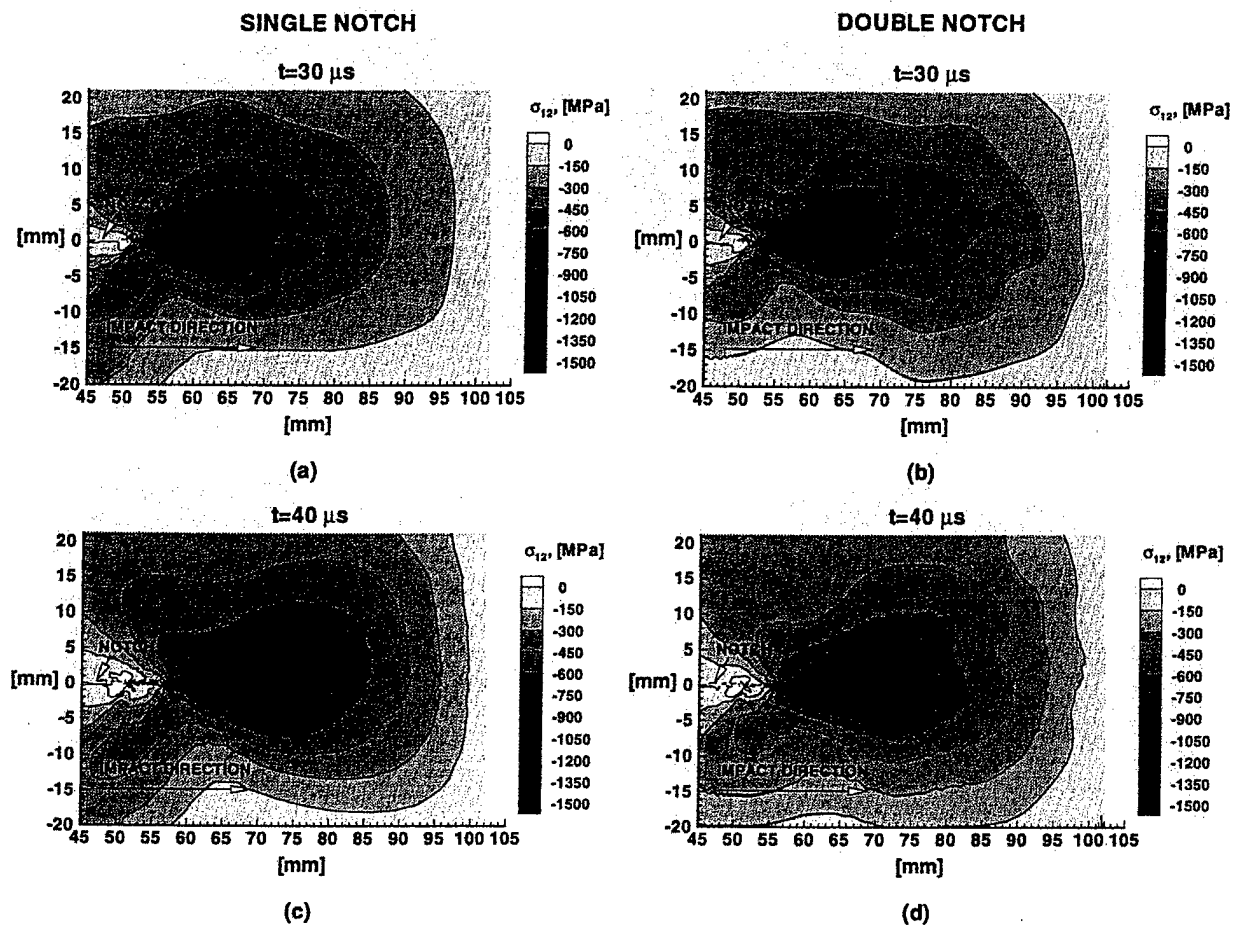


**Figure 5** Comparison of the distributions of in-plane shear stress ( $\sigma_{12}$ ) in singly and doubly notched specimens loaded with a projectile having a velocity of  $25 \text{ m s}^{-1}$ .

#### 4. References

1. Kaltoff, J.F., Shadow Optical Analysis of Dynamic Shear Fracture, *SPIE*, vol. 814, *Photomechanics and Speckle Metrology*, pp. 531-538 (1987).
2. Kaltoff, J.F. and Winkler, S., Failure Mode Transition at High Rates of Shear Loading, in *Impact Loading and Dynamic Behavior of Materials* (edited by C.Y. Chiem, H.-D. Kunze and L.W. Meyer) Verlag, 1, pp. 185-195 (1987).
3. Mason, J.J., Rosakis, A.J. and Ravichandran, G., Full Field Measurements of the Dynamic Deformation Field Around a Growing Adiabatic Shear Band at the Tip of a Dynamically Loaded Crack or Notch, *J. Mech. Phys. Solids*, **42**, pp. 1679-1697 (1994).
4. Zhou, M., Rosakis, A.J. and Ravichandran, G., Dynamically Propagating Shear Bands in Pre-notched Plates: I – Experimental Investigations of Temperature Signatures and Propagation Speed, *J. Mech. Phys. Solids* **44**, 981 (1996).
5. Zhou, M., Ravichandran, G., and Rosakis, A.J., Dynamically Propagating Shear Bands in Pre-notched Plates: II – Finite Element Simulations, *J. Mech. Phys. Solids* **44**, 1007 (1996).
6. Zhou, M., Needleman, A. and Clifton, R.J., Finite Element Simulations of Dynamic Shear Localization in Plate Impact, *J. Mech. Phys. Solids*, **42**, pp. 423-458 (1994).
7. Moran, B. and Shih, C.F., Crack Tip and Associated Domain Integrals from Momentum and Energy Balance, *Engin. Fract. Mech.*, **27**, pp. 615-642 (1987).
8. Moran, B. and Shih, C.F., A General Treatment Crack Tip Contour Integrals, *Int. J. Fract.*, **35**, pp. 295-310 (1987).